Journal of Engineering Physics and Thermophysics, Vol. 70, No. 4, 1997

HEAT TRANSFER AND PLASMATRON ELECTRODE EROSION

A. Marotta[a], L. I. Sharakhovsky[a], and V. N. Borisyuk[b]

UDC 621.387.143.014.31

A simple thermophysical model is proposed for cold electrode erosion in electric-arc heaters. The model regards erosion as characterized by an effective enthalpy for the change of state of the electrode material in the arc spot from solid to plasma. We show that the erosion problem can be represented by a system of three one-dimensional equations. The total heat flux in the arc spot can be represented by the electrode voltage drop. A magnetically driven arc rotating between copper ring electrodes was used for the experiments. The present model enables us to reveal the relative significance of the different parameters in the erosion process and to predict the erosion behavior in cold-electrode electric-arc heaters over a wide range of parameters.

1. INTRODUCTION

Cold-electrode electric-arc heaters have many potential applications in different areas of technology. However, the lifetime of arc heaters is seriously limited by the erosion of the electrodes, mainly the copper cathode, hindering their wide application in industry. To prevent their fast destruction by erosion, cold electrodes must be operated with fast moving arc attachments, provided by a magnetic field or a swirling gas. For a long time, it has been considered that the main role in the erosion of copper electrodes was played by complex physical-chemical processes in the oxide layers of the electrodes surfaces. Much progress has been achieved by Guile et al. in showing experimentally that the basic mechanism in the erosion rate of oxide-covered electrodes was dominated by fusion of the substrate metal [1]. They proposed an Arrhenius-type relationship for the calculation of erosion [1]:

$$dm/dT = A \exp - (\Delta G_{er}/kNT) ,$$

where dm/dT is the mass erosion rate, A is the "rate factor," ΔG_{er} is the erosion reaction activation energy, k is Boltzmann's constant, N is Avogadro's constant, and T is the electrode surface temperature. The value of ΔG_{er} was found by Guile et al. to be rather close to the activation energy for interatomic bond "loosening" (fusion) of the substrate material. In this paper, a theoretical model is presented that is based on the same fusion thermophysical concept and applied to our and other authors' experimental data, showing that the model is able to take account of the main features of the copper electrode erosion process [2-5].

2. THEORY

If current density in the arc spot does not exceed 10^7 A/cm^2 (for copper, 10^8 A/cm^2), Joule heating of the electrode material under the arc spot can be neglected [6]. In this case, we can imagine the arc spot replaced by an ideal circular heat source with uniformly distributed heat flux density $q_0 = jU = \text{const}$ [2-4, 6], where j is the arc spot current density and U we call the volt-equivalent of the arc spot heat flux (it is defined as the relation between the integral heat flux input to the arc spot and the arc current and is measured with the aid of a special experimental setup). We, then, study the heating of the electrode surface in coordinates attached to and moving with the source with constant velocity v (see Fig. 1). The maximum time of a given electrode point heat exposure

[a]Instituto de Física "Gleb Wataghin," Universidade Estadual de Campinas, São Paulo, Brasil, [b]Luikov Heat and Mass Transfer Institute, Minsk, Belarus. Published in Inzhenerno-Fizicheskii Zhurnal, Vol. 70, No. 4, pp. 551-559, July-August 1997. Original article submitted March 18, 1997.

 1062-0125/97/7004-0550$18.00

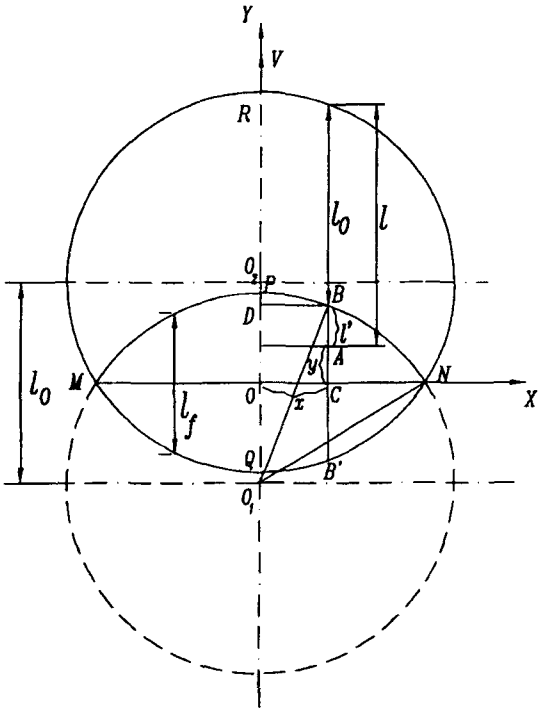

Fig. 1. Schematic diagram of the arc spot heat source: MRNPM – zone below the melting temperature T_f; MPNQM – fusion zone.

to the arc spot is equal to $\tau_{max} = d/v$, where d is the arc spot diameter and v is the arc velocity. Due to the high arc velocities, the Fourier number $Fo_d = a\tau_{max}/d^2 \ll 1$ [4-6], where a is the electrode thermal diffusivity. Taking into account that $d \ll b$, or $Fo_b = a\tau_{max}/b^2 \ll 1$, where b is the thickness of the electrode wall, we solve for a semi-infinite body ($0 \leq z < \infty$) and for $\tau > 0$ the one-dimensional heat conduction problem under the condition $q_0 = \text{const}$; for $\tau = 0$, $z = 0$ and $z = \infty$, we take respectively, $T(z, 0) = T = \text{const}$, $q_0 = -\lambda \partial T(0, \tau)/\partial z$ and $\partial T(\infty, \tau)/\partial z = 0$, where λ is the thermal conductivity of the electrode material, and z is perpendicular to the electrode surface. The solution of this problem is given by the equation [7, 8]:

$$T(z, \tau) = T + \frac{2q_0}{\lambda} \sqrt{a\tau}\ \text{ierfc}\left(\frac{z}{2\sqrt{a\tau}}\right). \tag{1}$$

Making $T(0, \tau_0) = T_f$, we obtain the time required for the electrode surface to reach the fusion temperature T_f:

$$\tau_0 = \frac{\pi}{4a}\left[\frac{(T_f - T)\lambda}{q_0}\right]^2. \tag{2}$$

For points in the electrode surface that lag behind the arc spot front edge by a distance of $l < l_0$ ($l_0 = v\tau_0$ (see Fig. 1), the temperature of the electrode beneath the heat source is determined by equation (1), and heat removal Q_r through heat conduction into the electrode body is equal to the arc spot heat input Q_0. Starting at $\tau = \tau_0$ (line MPN in Fig. 1), for points whose distance $l \geq l_0$, i.e., within the area MPNQM (the fusion area), the temperature $T = T_f = \text{const}$. We use the parameter $f = l_0/d = \tau_0 v/d$ to characterize the fusion zone extent in the arc spot. It is easy to see that f can be written in the following form:

$$f = \frac{\pi^{1.5} v \lambda^2 (T_f - T)^2}{8aj^{1.5}U^2 I^{0.5}}, \tag{3}$$

if we replace d by $2\sqrt{I/\pi j}$, τ_0 by (2) and q_0 by jU, where I is the arc current.

If we take the hypothesis that the erosion mass originates in the fusion zone and that the mass erosion rate G (kg/sec) is proportional to the "erosion heat" Q_{er} [4] (heat spent in transforming the electrode mass in the fusion zone from the solid state into the plasma one), we can write:

$$Q_{er} = Q_0 - Q_r = h_{ef} G = h_{ef}\, gI\,, \tag{4}$$

where h_{ef} is the erosion effective enthalpy and g is the specific erosin rate (kg/C).

Our aim is to calculate Q_r and Q_0 in the fusion zone. Neglecting the thickness of the liquid layer and assuming $T = T_f$ at $z = 0$, the heat conduction problem for the fusion zone can be solved for $\tau > \tau_0$, with equation (1) as the initial condition at $\tau = \tau_0$. The solution of this problem gives the heat flux density which is removed through the fusion zone [9]:

$$q_r = \frac{2q_0}{\pi} \tan^{-1} \sqrt{\left(\frac{\tau_0}{\tau - \tau_0} \right)}\,. \tag{5}$$

We integrate (5) over all the fusion zone area. After some substitutions and simplifications, the integral of (5) yields:

$$Q_r = -\, 4q_0 r^2 f\beta + \frac{8q_0 r^2 \beta}{\pi} \left[\sqrt{f}\, w_1 + w_2 \right], \tag{6}$$

where r is the spot radius, x and y are coordinates of the arbitrary point A in Fig. 1 and $w_1 = \int_0^1 \sqrt{\gamma(p) - f}\, dp$, $w_2 = \int_0^1 \gamma(p) \tan^{-1}(\sqrt{f}/\sqrt{\gamma(p) - f})\, dp$, $\beta = \sqrt{1 - f^2}$, $p = x/r\sqrt{1 - f^2}$ and $\gamma(p) = \sqrt{1 - p^2(1 - f^2)}$.

The integral heat flux input in the fusion zone area Q_0 can be expressed as being proportional to its area F_{MPNQM} (see Fig. 1). Accordingly, we obtain

$$Q_0 = 2q_0 \int_0^{\sqrt{r^2 - l_0^2/4}} (2\sqrt{r^2 - x^2} - l_0)\, dx = 2q_0 r^2 (\sin^{-1} \beta - f\beta)\,. \tag{7}$$

Taking into account the above equations yields:

$$Q_{er} = UIW = U_{er} I = (h_{ef}\, g)\, I\,, \tag{8}$$

where $U_{er} = UW$ we call the volt-equivalent of the erosion heat and W is a function of the f parameter, is given by:

$$W = \frac{2}{\pi} \left[\sin^{-1} \beta + f\beta - \frac{4}{\pi} \beta \left(\sqrt{f}\, w_1 + w_2 \right) \right], \tag{9}$$

which can be approximated by a rather simple expression:

$$W \approx W' = 1 - f \left(\frac{7.13}{2.475 + f} + \frac{0.442}{0.04 + f} - 1.477 \right). \tag{10}$$

The standard deviation of (10), with respect to (9), is equal to 0.011 ($W_{max} = 1$). From (8) we obtain the expression for the specific erosion rate [4],

$$g = \frac{UW}{h_{ef}}\,. \tag{11}$$

In (8) we note that U_{er} is a linear function of g, i.e., $U_{er} = h_{ef} g$. This equation will be usefull when comparing the erosion experimental data with the present theory, where we should make the constraint $U_{er} = 0$ for all points

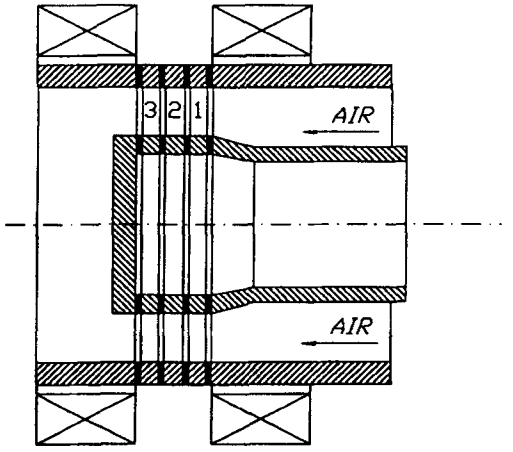

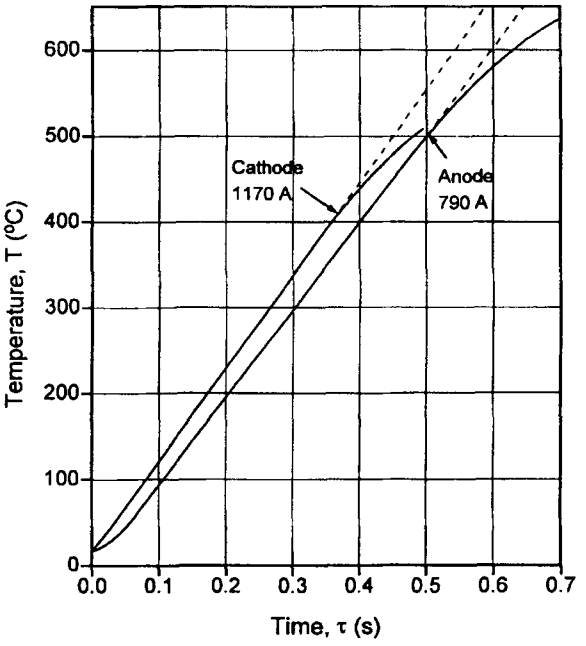

Fig. 2. Scheme of the experimental setup for measuring the volt-equivalent of the arc spot heat flux U and the arc spot current density j. 1) current-fed rings; 2, 3) electroneutral rings.

Fig. 3. Oscillogram records of the temperature of the ring electrodes versus time. The arrow position corresponds to the critical regime when $dT/d\tau$ starts to drop (beginning of electrode fusion).

giving $f \geq 1$, as for these points, $g = 0$. As a matter of fact, there is observed in different experiments some minimum erosion level for $f \geq 1$, which we take into account by introducing the term g_0 (called microerosion) into equation (11), giving for g, the final expression [4]:

$$g = g_0 + \frac{UW}{h_{ef}} = g_0 + \frac{U_{er}}{h_{ef}}. \tag{12}$$

From the above results, we see that the thermophysical model can be represented, in the simpliest form, by the system of three equations (3), (9) or (10), and (12). The main specifying parameters for calculating the total specific erosion g are the current I, the arc velocity v, and the electrode surface temperature T.

3. EXPERIMENTAL INVESTIGATIONS

3.1. Experiments on U and j. A coaxial experimental setup (Fig. 2) with uncooled copper rings as electrodes and a magnetically driven arc was used for thermal measurements of the volt-equivalent of the arc spot heat flux U and current density j. U was measured using an nonstationary method: a thermocouple records the heating curve of the electrode surface temperature as function of time (see Fig. 3). From the slope $dT/d\tau$ of the linear portion of this curve we calculate U. Details of the experiments are described elsewhere [5]. Table 1 shows the measured values of U and a comparison between $U_c + U_a$ and the sum of cathodic and anodic near-electrode voltage drops $\Delta U_c + \Delta U_a$ (this last one, measured by a conventional method). A linear dependence of U (in volts) on magnetic field strength B (in Tesla) for atmospheric pressure is obtained:

$$U = 6.52 + 4.28B. \tag{13}$$

Two methods were used for the measurements of j: an nonstationary and a stationary method. For the first one, we used the same experimental setup (Fig. 2) as for U. The parameter $j$can be obtained by reading the temperature

TABLE 1. Cathode and Anode Arc Spot Parameters for Different Experimental Conditions. Data in Brackets and Without Brackets Were Obtained by Different Procedures (see [5])

B, T	P, atm	U_c, V	U_a, V	$\Delta U_c + \Delta U_a$, V	$U_c + U_a$, V
0.133	1	6.8 (7.5)	10.9 (11.4)	18	17.7 (18.9)
0.133	8	9.4 (10.1)	10.4 (11.4)	22	19.8 (21.5)
0.133	20	10.2	11.4 (10.6)	–	21.6
0.50	40	(12.5)	–	–	–
0.24	1	7.4	–	–	–
0.95	1	10.6	13.7 (14.4)	27	24.3

TABLE 2. Anode and Cathode Arc Spot Current Densities j and Arc Spot Diameters d for Different Experimental Conditions Obtained by Nonstationary Method (see [5])

I, A	v, m/sec	T, K	d, mm	j, A/cm^2
		Cathode		
1170	226	797	1.08	$1.28 \cdot 10^5$
1140	239	817	1.07	$1.27 \cdot 10^5$
1377	260	874	1.27	$1.08 \cdot 10^5$
1410	289	947	1.39	$0.93 \cdot 10^5$
		Anode		
1170	226	933	1.85	$0.43 \cdot 10^5$
1170	226	941	1.87	$0.42 \cdot 10^5$
790	189	886	1.41	$0.51 \cdot 10^5$
1172	265	916	1.71	$0.51 \cdot 10^5$
790	189	953	1.56	$0.41 \cdot 10^5$

T, where the slope $dT/d\tau$ of the straight line of the thermocouple heating curve versus time mentioned above begins to drop (see Fig. 3) [5]. This drop indicates the beginning of electrode melting at the arc spot. We obtain the arc spot current density by making $f = 1$ in equation (3). This yields the following equation:

$$j = \frac{\pi}{4}\left[\frac{\lambda^4}{a^2}\frac{v^2 (T_f - T)^4}{U^4 I}\right]^{1/3}, \tag{14}$$

Current densities calculated in accord with (14) are presented in Table 2. The stationary method for measuring j will be described in the next section, together with the erosion measurements.

3.2. Erosion Experiments. A similar experimental setup (Fig. 2) to that used for the measurements of U and j, but equipped with water-cooled commercial copper ring electrodes, was used for the cathode erosion measurements in magnetically driven arcs. Compressed undehumidified atmospheric air was used as the working gas. The mass erosion rate was measured by the weighting method. The details of the experimental procedure are described elsewhere [5]. The experiments were realized for two values of the inner ring electrode diameters D_1: 50 and 90 mm. The range of variation of the main parameters was the following: $I = 24.5-1000$ A, $v = 19.3-344$ m/sec, $T = 300-1073$ K, $B = 0.03-0.242$ T, $g = 6.3 \cdot 10^{-10}-4.2 \cdot 10^{-8}$ kg/C, where B is the magnetic field strength.

TABLE 3. Cathode Arc Spot Current Densities j and Arc Spot Diameters d for Different Experimental Conditions Obtained by Stationary Method [5]

I, A	v, m/sec	T, K	U, V	d, mm	j, A/cm^2
360	110	633	7.09	0.55	$1.53 \cdot 10^5$
370	67.4	507	6.65	6.57	$1.47 \cdot 10^5$
375	62.0	585	6.65	0.63	$1.23 \cdot 10^5$
395	65.5	472	6.65	0.58	$1.49 \cdot 10^5$
400	111.2	660	7.09	0.60	$1.41 \cdot 10^5$
440	66.0	577	6.65	0.68	$122 \cdot 10^5$
450	128.6	692	7.09	0.64	$1.40 \cdot 10^5$
490	63.8	535	6.65	0.71	$1.24 \cdot 10^5$
495	55.0	563	6.65	0.77	$1.07 \cdot 10^5$
705	81.0	472	6.65	0.80	$1{,}42 \cdot 10^5$
725	80.0	485	6.65	0.82	$1.37 \cdot 10^5$
765	87	460	6.65	0.81	$1.47 \cdot 10^5$

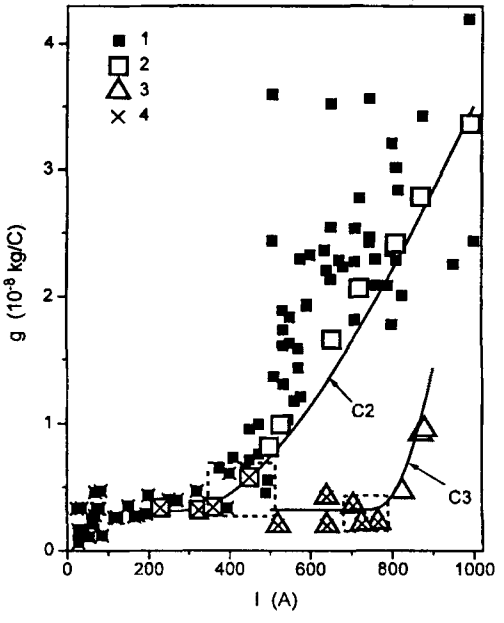

Fig. 4. Specific cathode electrode erosion g vs current I: 1, 2) cathode with inner ring diameter $2R_1$ = 50 mm; 3) cathode with inner ring diameter $2R_1$ = 90 mm; 4) points with $f > 1$; C2, theoretical curve for experimental points 2; C3, theoretical curve for experimental points 3.

A stationary experiment was carried out consisting in the registration of the inner, heated by the arc, electrode ring surface temperature T, the arc velocity v, the current I, the integral heat flux Q supplied to the inner ring electrode surface, and the change in weight of the eroded ring during the experiment (measurement of G or g). The total heat flux Q was obtained by cooling water calorimetric measurements.

3.3. Erosion Experimental Results. Experimental data (108 points) on the specific erosion g versus the arc current I for the cathode erosion are presented in Fig. 4. We observe a strong increase in the erosion intensity,

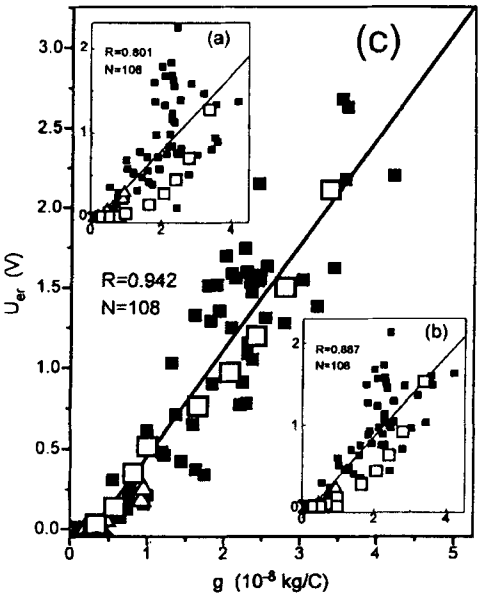

Fig. 5. Volt-equivalent of cathode erosion heat U_{er} vs specific erosion g: a) for average values $U = 6.78$ V and $j = 1.35 \cdot 10^{-9}$ A/m^2; b) for $U = f(B)$ in accord with equation (15) and average value $j = 1.35 \cdot 10^{-9}$ A/m^2; c) for $U = f(B)$ and $j = f(B)$ in accord with equations (15) and (17), respectively.

beginning at some critical current value, which depends on the value of the electrode diameter. For the electrode with the 90-mm diameter, erosion begins to increase at higher currents than for the 50-mm ring diameter (compare the two groups of points enclosed in frames in Fig. 4).

Assuming that the abrupt increase in erosion at the critical current value is due to the fusion onset in the arc spot ($f = 1$), it is possible to estimate the arc spot current density (stationary method of measuring arc spot current density) [5] using formula (14) for the points inside the frames in Fig. 4. Values of the arc spot current densities for these points are given in Table 3. The average value is equal to $j = 1.35 \cdot 10^9$ A/m^2.

The minimum erosion value g_0 (microfusion erosion) corresponds to $f > 1$ [4, 10]. This value can be estimated from Fig. 4 as 2.5–3 μg/C, approximately, for points marked as crosses (with $f > 1$). From processing of experiments in the form $U_{er} = f(g)$ we can derive more accurate averaged values for g_0 and h_{ef}, as follows from equation (12). In order to reject points pertaining to the onset of erosion ($f = 1$), and also points pertaining to the minimum of erosion ($f > 1$), we applied the constraint $U_{er} = 0$ for all points with $f \geq 1$. The plot $U_{er} = f(g)$ is shown in Fig. 5a, where we used the average values $j = 1.35 \cdot 10^9$ A/m^2 and $U = 6.78$ V for all experimental points. For the best linear fitting equation $U_{er} = A + Bg$, we obtained a correlation coefficient $R = 0.801$. However, if we take into account the dependence of U on the magnetic field B, in accord with (13), the correlation coefficient improves appreciably ($R = 0.887$), with $h_{ef} = 49.6 \pm 2.5$ MJ/kg and $g_0 = (2.81 \pm 0.85) \cdot 10^{-9}$ kg/C (see Fig. 5b).

Returning to Fig. 4, we highlight two groups of points (for the cathode diameters) $D_1 = 50$ mm and $D_1 = 90$ mm). The distinguishing feature of each of the groups of points is that all the controlling parameters (the magnetic field, the air flow rate, and the cooling-water mass flow rate) remained constant. The magnetic fields for the cathode diameters 50 and 90 mm were, respectively, $B = 0.133$ T and $B = 0.03$ T. For each of these groups, we plotted experimental values of electrode temperature and arc velocity versus current. Then, these were approximated by analytical expressions $T = f(I)$ and $v = f(I)$.

In Fig. 4, we plot the theoretical functions $g(I)$ (curves C2 and C3) for the highlighted data, in accord with equations (3), (10), and (12), taking account the analytical approximations $T = f(I)$, and $v = f(I)$, mentioned above. Due to the different magnetic field intensities used for the two groups, the value of the arc spot current density was chosen individually for each group of points to obtain value $f = 1$ at the corresponding region of abrupt erosion increase (points in frames) and the best theoretical line for the remaining points at $f < 1$. This gives, for the first

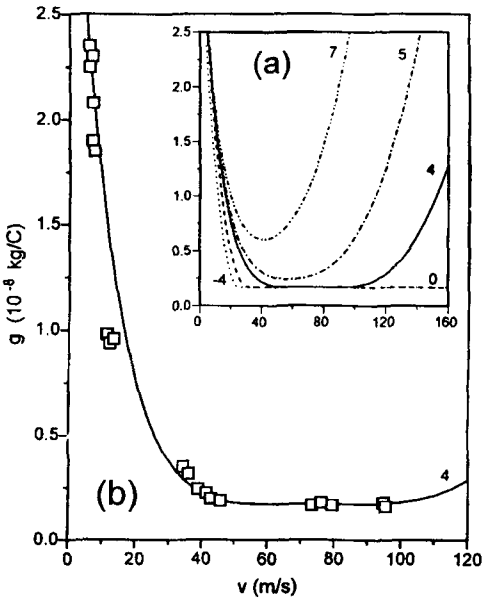

Fig. 6 (a) Theoretical specific erosion g vs arc velocity v for different values of dT/dv (Ks/m) (shown) for I = 100 A, T_0 = 480 K, h_{ef} = 130 MJ/kg; b) experimental data taken from [11].

group (B = 0.133 T), $j \simeq 1.62 \cdot 10^9$ A/m^2, and for the second one (B = 0.03 T), $j \simeq 1.36 \cdot 10^9$ A/m^2. Then, the following expression can be derived:

$$j = (1.282 + 2.6B) \cdot 10^9 , \tag{15}$$

where j is given in A/m^2 and B in teslas.

Substitution of (13) for $U(B)$ and (15) for $j(B)$ in (3) and then in (10) results in a much better agreement of the theoretical straight line function $U_{er} = f(g)$ with the experimental data shown by the two groups of highlighted points (see Fig. 5c). The best-fit straight line in Fig. 5c gives a correlation coefficient R = 0.942, $h_{ef} \simeq 66.1 \pm 2.3$ MJ/kg and $g_0 \simeq (3.12 \pm 0.58) \cdot 10^{-9}$ kg/C.

The two theoretical curves C2 and C3 for the two groups of highlighted experimental data in Fig. 4 are shown taking into account the obtained above values h_{ef} = 66 MJ/kg and $g_0 = 3.1 \cdot 10^{-9}$ kg/C. As one can see in Fig. 4, the theoretical curves show a rather good agreement with the corresponding highlighted groups of experimental points. The same groups of points are also highlighted in Figs. 5a, 5b, and 5c. We see from the last figures that the deviation of these groups of points from the fitted lines decreases progressively as the U and j dependences on the magnetic field are taken into account.

In a gasdynamically driven arc, the colder gas tends to flow closer to the electrode wall with an increase of the swirl velocity, resulting in a decrease in the electrode temperature, i.e., $dT/dv < 0$, if we take a linear dependence $T = T_0 + v(dT/dv)$ of electrode temperature on arc velocity, where T_0 is the initial electrode temperature and dT/dv = const. For a magnetically driven arc, the gas velocity tends to lag behind the arc velocity, which causes gas disturbances and increased heat transfer to the electrode. This leads to an increase in the electrode surface temperature, resulting in $dT/dv > 0$.

Fig. 6a shows theoretical plots of the erosion behavior with increasing arc velocity. For $dT/dv < 0$ (gasdynamic case), the dependence is trivial: higher velocity, less erosion. However, for $dT/dv > 0$ (magnetically driven arc), there is a range of arc velocities for which the specific erosion decreases, attains some minimal level $g \geq g_0$, and then increases with increasing velocity.

In Fig. 6b we give a qualitative comparison of the theoretical behavior of erosion with an increase in the velocity of the arc using experimental data presented in [11]. This comparison is qualitative, since the authors do not communicate the temperature conditions of the copper cathode. We selected the average values U = 6.7 V and $j = 1.41 \cdot 10^9$ A/m^2 for a magnetic field of 0.05 T according to (13) and (15). We used $g_0 = 1.7$ μgC^{-1} for the

minimum level of erosion, as noted in [11]. We assumed $T = 480$ K, so that $f = 1$ is obtained at the minimum level g_0. With $dT/dv = 4$ and $h_{ef} = 130$ MJ/kg, a good qualitative agreement of the theoretical curve with the experimental data is obtained. As can be seen in Fig. 6b, with a further increase in velocity it is possible to expect an increase in the erosion. Unfortunately, the authors do not give experimental points in this region. We note that the obtained values of h_{ef} and g_0 differ quite markedly from the ones extracted from our experiments: 130 MJ/kg and $1.7 \cdot 10^{-9}$ kg/C, respectively, for their experiments. This difference could be explained by the different cathode materials and working gases: while we used commercial copper and undehumidified compressed atmospheric air, they used [11] electrolytic copper and pure argon-nitrogen mixtures, respectively.

CONCLUSION

We have demonstrated that our and other authors' experimental results on copper electrode erosion are resonably explained by a thermophysical model. By plotting the volt-equivalent of the erosion heat U_{er} calculated from experimental data as a function of the experimentally measured specific erosion g we were able to obtain the main parameters of the erosion behavior, g_0 and h_{ef}. We have shown data on the volt-equivalent of the arc spot heat flux and on the arc spot current density, measured by thermal methods. These measurements have demonstated that these parameters are functions of the magnetic field strength in magnetically driven arcs. We were able also to explain an unexpected behavior of the erosion, observed by different authors, when, increasing the magnitude of magnetic field, at first, the erosion decreases, attains or stabilizes at a certain minimum level, and then starts increasing. In conclusion, a thermophysical model of copper-electrode erosion under the action of a fast moving arc spot has been realized. Simple equations have been obtained that enable one to predict the level of electrode erosion on the basis of the main parameters of electric arc heaters.

We thank Mr. A. A. B. do Prado and Mr. J. B. Pinheiro for their technical assistance in this work. We acknowledge the financial support of CNPq, FAPESP and FINEP of Brazil.

REFERENCES

1. A. E. Guile, A. H. Hitchcock, K. Dimoff, and A. K. Vijh, J. of Phys. D: Appl. Phys., 15, 2341-2355 (1982).
2. L. I. Sharakhovsky, A. Marotta, V. N. Borisyuk, and L. O. M. da Silva, "A new thermophysical model for cold electrodes erosion," in: Proc. of 12th Int. Symp. on Plasma Chem. (eds. J. V. Heberlein, D. W. Ernie, and J. T. Roberts), Minneapolis, Minnesota, USA, University of Minnesota (1995), pp. 1595-1600.
3. L. I. Sharakhovsky, A. Marotta, V. N. Borisyuk, and L. O. M. da Silva, "A thermophysical model for cold electrode erosion in the form of a Guile-Arrhenius relationship," in: Proc. of XXII Int. Conf. on Phen. on Ionized Gases (eds. K. H. Becker, W. E. Carr, and E. E. Kunhardt), Hoboken, USA, Stevens Inst. of Tech. (1995), pp. 159-160.
4. A. Marotta and L. I. Sharakhovsky, "A theoretical and experimental investigation of copper electrode erosion in electric arc heaters, part 1: the thermophysical model," J. of Phys. D: Appl. Phys., 29, 2395-2403 (1996).
5. L. I. Sharakhovsky, A. Marotta, and V. N. Borisyuk, J. of Phys. D: Appl. Phys. (1996), to be published.
6. A. V. Luikov, A. V. Borovchenko, V. I. Krylovich, V. V. Toropov, L. I. Sharakhovsky, and A. S. Shaboltas, "Heat transfer in near-electrode region of the blown electric arc," in: Proc. of JSME 1967 Semi-Int. Symp., Tokyo, Sept. 4-8 (1967), pp. 113-119.
7. H. S. Carslaw and J. C. Jagger, Conduction of Heat in Solids, London: Oxford (1959).
8. A. V. Luikov, Analytical Heat Diffusion Theory, New York and London: Acad. Press (1968).
9. V. I. Krylovich and A. S. Shaboltas, Izv. Akad. Nauk BSSR , Ser. Fiz.-Energet. Science, 1, 93-98 (1973).
10. L. I. Sharakhovsky, A. Marotta, and V. N. Borisyuk, J. of Phys. D: Appl. Phys. (1996), to be published.
11. R. N. Szente, R. J. Munz, and M. G. Drouet, J. of Phys. D: Appl. Phys., 20, 754-756 (1987).